

Interacting triplons in frustrated spin ladders: Binding and decay in BiCu_2PO_6

Leanna B. Müller¹ and Götz S. Uhrig^{1,*}

¹*Condensed Matter Theory, TU Dortmund University, Otto-Hahn-Straße 4, 44227 Dortmund, Germany*
(Dated: November 16, 2022)

Establishing a comprehensive model of the rich spin dynamics in BiCu_2PO_6 has been a challenge over the last decade. Inelastic neutron scattering experiments revealed that its elementary triplons are non-degenerate showing the existence of significant anisotropic spin couplings. Evidence for triplon decay into two triplons has been found, but two prominent downturns in the dispersions eluded an explanation. Level repulsion due to hybridization of single triplons with the continuum of two-triplon scattering states has been proposed as explanation. We show that this concept may explain the weak downturn at higher energies, but fails for the most pronounced downturn at lower energy. In turn, we provide evidence that this downturn is the signature of a two-triplon bound state of essentially singlet character pointing to triplon-triplon interaction as the second crucial ingredient of the spin dynamics in this exemplary system.

I. INTRODUCTION

Strongly correlated quantum systems are notoriously difficult to understand due to the extremely fast growth of dimensionality of the relevant Hilbert space with system size. At low energies close to the ground state, however, the situation is much more favorable. Elementary excitations can be identified in terms of which most physical properties can be explained; they can be addressed as particles or quasiparticles of the system. For translationally invariant systems, i.e., in crystals, the dispersion $\hbar\omega(\vec{k})$ yields the energy dependence on the momentum $\hbar\vec{k}$ of the quasiparticles. Theoretically, this is described by a diagonal Hamiltonian which is bilinear in creation and annihilation operators. In addition, these excitations can decay, for instance one excitation into two excitations which is captured by trilinear terms in the Hamiltonian. The pairwise interaction of two particles, called two-particle interaction, is described by quadrilinear terms. Terms and processes involving even more quasiparticles may also arise and can be denoted by quintilinear terms and sextilinear terms (three-particle interactions) and so on. These higher interactions are rarely considered, but they do occur in effective models and can lead to important shifts of spectral weight and even bound states [1].

Here we focus on systems formed by localized spins in insulators which are called quantum magnets. Generically, they provide clean and well-defined systems which are only weakly coupled to other degrees of freedom such as charges or phonons. Thus, the elementary excitations are long-lived unless they decay intrinsically due to terms beyond the bilinear ones. Omnipresent pairwise interactions can lead to bound states. Hence, quasiparticle decay and binding are the two foci of the present Letter which we discuss in the particular system BiCu_2PO_6 realizing weakly coupled spin ladders [2].

There are three large classes of elementary excitations of quantum magnets. In systems with long-range magnetic order the elementary excitations are quantized spin waves, so called magnons. In low-dimensional or very strongly correlated systems fractional excitations occur called spinons. In gapped

quantum antiferromagnets without order the elementary excitations above the $S = 0$ ground state have triplet character with $S = 1$ and are called triplons [3] to underline their quasiparticle nature. For BiCu_2PO_6 , these triplons are the relevant elementary excitations [4–7]

Theoretically, quasiparticle decay and its preconditions have been discussed generally [8, 9] and for magnetic excitations in particular [10–14]. Experimentally, it has been observed in a number of ordered quantum magnets [15–17] and disordered quantum magnets [5, 18, 19] underlining the relevance of the issue. The decay of magnons is particularly strong if a single magnon can decay into two magnons as is the case for non-collinear ordering, for instance in triangular quantum antiferromagnets [14, 16, 20–23]. A noteworthy observation is that the trilinear terms also imply a renormalization of the energy of the single magnon by level repulsion. For large enough trilinear terms the dispersion is pushed below the multiparticle continuum so that no decay occurs anymore; this has been dubbed “avoided quasiparticle decay” [14]. Generically, it is also seen in one-dimensional systems [11, 12, 14]. Similarly, decay processes from one quasiparticle to three quasiparticles also lead to a renormalization of the dispersion due to level repulsion as seen in the collinear square lattice Heisenberg antiferromagnet [24–26].

Binding stems from the quadrilinear terms as explained above. In quantum ferromagnets the fully polarized state is the ground state and the number of magnons is conserved in the model as given. Since long, bound states of magnons in ferromagnets are established [27–30] and play a role in current applications [31]. For quantum antiferromagnets, the situation has more facets depending on the nature of the ground state. For unfrustrated antiferromagnets with long-range order, bound states of two magnons appear in gapped, easy-axis systems [26, 32–34] which disappear on passing to the isotropic antiferromagnet. But there remains a strong attractive force which shifts spectral weight to lower energies and induces a roton-like minimum in the magnon dispersion by level repulsion [24, 25].

In one dimension, no long range order occurs without spin anisotropies in the Hamiltonian. But fractional spinon excitations are established [35] which also form bound states [27, 36, 37]. They could be experimentally verified only re-

* goetz.uhrig@tu-dortmund.de

cently [38]. We point out that triplon excitation can be also seen as bound states of confined spinons [39, 40].

Gapped antiferromagnets with neither long-range order nor fractionalization are valence bond solids and their elementary excitations are triplons which generically attract each other, in particular if the total spin remains zero. This has been established for spin ladders [41–47], dimerized spin chains [48–51], and for the Shastry-Sutherland lattice [52–54], both in theory and experiment.

II. THE COMPOUND

In this Letter, we elucidate quasiparticle decay and binding in the strongly frustrated spin ladders in BiCu_2PO_6 . The crystal structure has been discussed by Tsirlin *et al.* [2], but for our purposes the spin model is sufficient. The spins $S = 1/2$ are localized at the copper ions which are positioned in tubes made from an upper and a lower spin ladder. In addition, the spin ladders are weakly coupled forming a two-dimensional lattice [55, 56]. Here only the topology of the magnetic exchange couplings matters so that we project the upper and lower spin ladders in one plane, see Fig. 1.

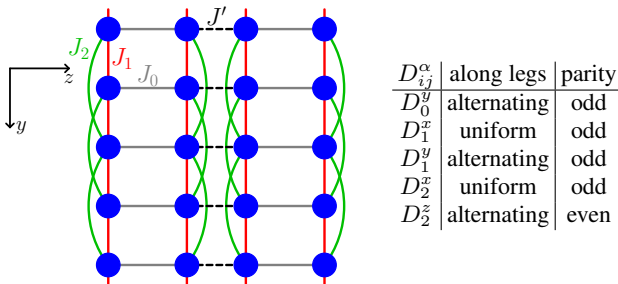


FIG. 1. Left: **Sketch of the spin model for BiCu_2PO_6** ; blue spheres denote the Cu^{2+} ions hosting the spins $S = 1/2$. The isotropic couplings J_0 , J_1 and J_2 define a single frustrated ladder while the isotropic interladder coupling J' weakly links adjacent ladders forming planes. Right: Sign of non-vanishing DM terms along the legs, parity w.r.t. reflection. The parity given for D_0^y refers to its term in the Hamiltonian, not to D_0^y itself.

The isotropic part of the Hamiltonian of a single frustrated spin ladder reads

$$\mathcal{H}_{\text{lad}} = J_0 \sum_i \mathbf{S}_i^L \mathbf{S}_i^R + J_1 \sum_{i,\tau} \mathbf{S}_i^\tau \mathbf{S}_{i+1}^\tau + J_2 \sum_{i,\tau} \mathbf{S}_i^\tau \mathbf{S}_{i+2}^\tau \quad (1)$$

with the rung index i and the $\tau \in \{\text{L}, \text{R}\}$ indicating the left or right leg, respectively. The interladder coupling J' is significantly weaker than the intraladder couplings, but not negligible [2, 4]. BiCu_2PO_6 represents a valence bond solid with triplons as elementary magnetic excitations because its spin system is gapped. Since the inversion symmetry about the Cu-Cu bonds is broken, anisotropic Dzyaloshinskii-Moriya (DM) couplings may occur [57] and were conjectured [2]. The splitting of the otherwise degenerate triplons [4, 5] clearly confirm this conjecture.

Including anisotropic couplings to our model of BiCu_2PO_6 we discuss the Hamiltonian

$$\mathcal{H} = \mathcal{H}_{\text{lad}} + \sum_{i,j} \mathbf{D}_{ij} (\mathbf{S}_i \times \mathbf{S}_j) + \sum_{i,j} \sum_{\alpha,\beta} \Gamma_{ij}^{\alpha\beta} S_i^\alpha S_j^\beta. \quad (2)$$

Note that we include the label $\{\text{L}, \text{R}\}$ indicating the leg of the ladder in the site indices i and j henceforth. In addition to \mathcal{H}_{lad} from Eq. (1) we consider the DM interactions $\mathbf{D}_{ij} (\mathbf{S}_i \times \mathbf{S}_j)$ and the symmetric anisotropic exchanges $\Gamma_{ij}^{\alpha\beta} S_i^\alpha S_j^\beta$. The sums with the site indices i and j are meant to count each pair of spins once. The couplings along the rungs of the spin ladder are labeled with the index 0, thus J_0 , \mathbf{D}_0 and $\Gamma_0^{\alpha\beta}$. The index 1 is used for all couplings between other nearest-neighbor (NN) sites, thus J_1 , \mathbf{D}_1 and $\Gamma_1^{\alpha\beta}$. Lastly, the couplings between next-nearest neighbor (NNN) sites are marked with the index 2, thus J_2 , \mathbf{D}_2 and $\Gamma_2^{\alpha\beta}$; see also Fig. 1. The symmetric anisotropic exchanges $\Gamma_{ij}^{\alpha\beta}$ represent the second order effects of the DM terms [58] reading

$$\Gamma_{ij}^\alpha = \frac{D_{ij}^\alpha D_{ij}^\beta}{2J_{ij}} - \frac{\delta^{\alpha\beta} \mathbf{D}_{ij}}{6J_{ij}} \quad (3)$$

and being defined such that the tensor Γ_{ij} is traceless [6]. The orientation of the \mathbf{D} vectors is determined by the selection rules based on the point group symmetries [57], see Fig. 1. The symmetry analysis [6] yields the results displayed on the r.h.s. of Fig. 1. Five DM components can assume finite values from which four components hold odd parity with respect to reflection about the center line of the spin ladder [46]. Hence they do not contribute to bilinear terms in the Hamiltonian, but only to trilinear and potential quintilinear terms.

III. THEORETICAL ANALYSES

The approach used extends the treatment in Ref. 6. We start from the isolated isotropic spin ladder which we map by continuous unitary transformation (CUT) [59, 60] to an effective model formulated in second quantization, i.e., in creation and annihilation operators of the elementary excitations, triplons [3, 40, 61]. The CUT takes the hardcore property of the triplons fully into account. This effective model conserves the number of triplons so that the computation of physical properties such as the dispersion, bound states, or spectral densities is greatly facilitated.

The CUT represents a systematic basis change and can be applied as well to any observable, in particular to the spin components $S_{i,\alpha}$. These transformed observables allow us to express all residual couplings (antisymmetric ($\propto \mathbf{D}_{ij}$) and symmetric DM terms ($\propto \Gamma_{i,j}^{\alpha\beta}$), interladder couplings ($\propto J'$) in terms for triplon operators. Since these additional couplings are small we ignore the hardcore property of the triplon operators in the subsequent step so that we can diagonalize the bilinear parts by a Bogoliubov transformation. This transformation is also applied to the trilinear terms ensuing from the odd parity DM terms. The quadrilinear terms are taken from the CUT of the isolated ladders and also subjected to

the Bogoliubov transformation. In view of the three momenta which can be varied freely in quadrilinear terms with momentum conservation this comprises a particularly large number of coefficients representing the numerical bottleneck in this calculation. From the resulting terms we keep the two-triplon interaction terms consisting of monomials of two creation and two annihilation operators. They are responsible for binding phenomena.

Finally, we compute resolvents in the hybridized one-triplon and two-triplon subspace at given total momentum $\hbar\mathbf{q}$. These resolvents provide access to the dynamic structure factor $S(\mathbf{q}, \omega)$ including sharp resonances outside the continuum of scattering states, see Appendix A. The momentum dependence of these sharp resonances is to be compared with the dispersion of the experimentally observed strong peaks. Sharp resonances can stem from either single triplon states which are renormalized by the hybridization with the two-triplon states or from bound two-triplon states.

a. Bilinear Level Previously, we performed the analysis of experimental inelastic neutron scattering (INS) data for BiCu_2PO_6 on the bilinear level and achieved best fits with the parameters $J_0 = 9.4\text{meV}$, $J_1 = 1.2J_0$, $J_2 = 0.9J_1$, $J' = 1.5\text{meV}$, $D_0^y = 0$, $D_1^x = 0.48J_1$, $D_1^y = 0.61J_1$, $D_2^x = 0$, and $D_2^z = -0.02J_2$. A figure showing the degree of agreement achieved is included in Appendix B; for details see Ref. [6]. Summarizing, the dispersions in the vicinity of the minima is captured well. But the downturns of the measured data remain completely unexplained. Additionally, the values of the NN DM terms are substantially larger than one is expecting for the relative strength of couplings stemming from spin-orbit coupling: 10 to 20% of the corresponding exchange coupling. Qualitatively, these findings agree with those by Hwang and Kim [7] for the bilinear model.

b. Trilinear Level This brings us to the trilinear terms resulting from the DM couplings of odd parity. As explained above, the trilinear terms introduce a new piece of physics, namely the decay of a triplon into two triplons and vice-versa the fusion of two triplons to a single one. In short, the one- and the two-triplon subspaces hybridize. The results are shown in Fig. 2. The dispersion branches around the minima are captured, but less well than on the bilinear level. This is due to the much more demanding numerical evaluation which does not allow us to scan all conceivable parameter combinations, for instance we stick to the ratios J_1/J_0 and J_2/J_1 determined on the bilinear level.

One satisfying observation underlining the importance of the trilinear terms is that the required DM couplings are much lower than on the bilinear level. The value for D_1^x has lowered from $0.48J_1$ to $0.25J_1$ and for D_1^y from $0.61J_1$ to $0.38J_1$ which brings them closer to the expected range of spin-orbit induced couplings. On the downside, however, we only find a weak feature of level repulsion in Fig. 2. There is a small downturn in the dispersion just before it enters into the scattering continuum at $k \approx 0.75$ r.l.u.. Comparing this feature to the significant experimental downturn at 7 meV it is evident that the hybridization due to trilinear terms is insufficient to explain the measured features. We stress that this conclusion agrees with the figures from previous calculations [7].

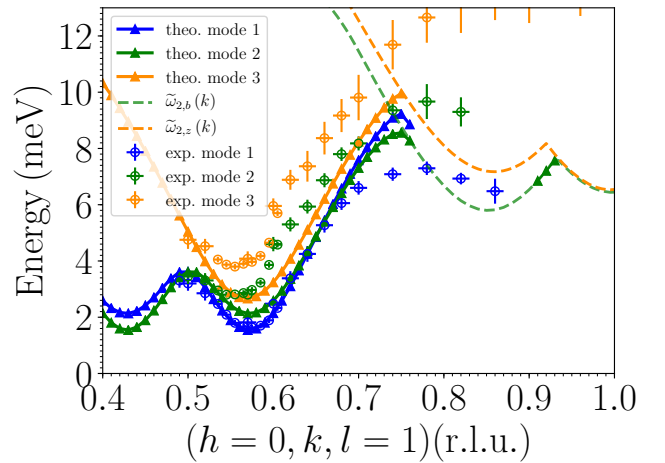


FIG. 2. **Dispersion in the trilinear model.** Energetically low-lying dispersion including the hybridization between the one- and the two-triplon states. A weak down-bending occurs before the single triplon dispersion enters the two-triplon continua at about $k = 0.75$ r.l.u.. The parameters used are $J_0 = 8.0\text{meV}$, $J_1 = 1.2J_0$, $J_2 = 0.9J_1$, $J' = 0.16J_0$, $D_0^y = 0.1J_0$, $D_1^x = 0.25J_1$, $D_1^y = 0.38J_1$, $D_2^x = 0.0$, and $D_2^z = -0.09J_2$. The dashed lines represent the lower edges of the two-triplon continua. The yellow curve is computed from the highest, yellow dispersion. The green one from the green dispersion. All other four continua edges lie between the two depicted continuum edges. Unlinked symbols are the experimental data from Ref. [5, 62].

We deduce that the level repulsion from the scattering continuum alone is too weak to account for the observed dispersions. This finding raises the question what generates the experimental features. Promising candidates are bound states since it is known that spin ladders host bound two-triplon states [41–47]. In addition, frustration enhances binding because the mobility of triplons is reduced while its interaction is enhanced [49–51].

c. Quadrilinear Level Describing the binding of two particles requires to include the quadrilinear terms in second quantization. First, we inspect the isolated ladder for which the CUT alone yields the effective model very reliably. Fig. 3 displays the dispersions of a single triplon and of the two bound states formed by two triplons. The latter are situated below the two-triplon band of scattering states shaded in light green-blue. It is remarkable that just at $k \approx 0.75$ r.l.u. the $S_{\text{tot}} = 0$ state, displayed by the red dotted curve, falls below the single triplon dispersion. This suggests that a bound state could indeed be involved in the experimental situation. A counterargument is that INS is sensitive only to $S = 1$ states, not to $S = 0$ states. While this holds in spin isotropic systems it does not apply in presence of the sizable spin anisotropies existing in BiCu_2PO_6 . For completeness, we also depict the bound $S = 1$ state by the grey dotted curve.

As next step, we compute the dynamic structure factor including the triplon-triplon interaction in the full 2D model in reciprocal space with in the Hilbert space spanned by one-triplon and two-triplon states at given total momentum. This is a very demanding calculation because the matrix represent-

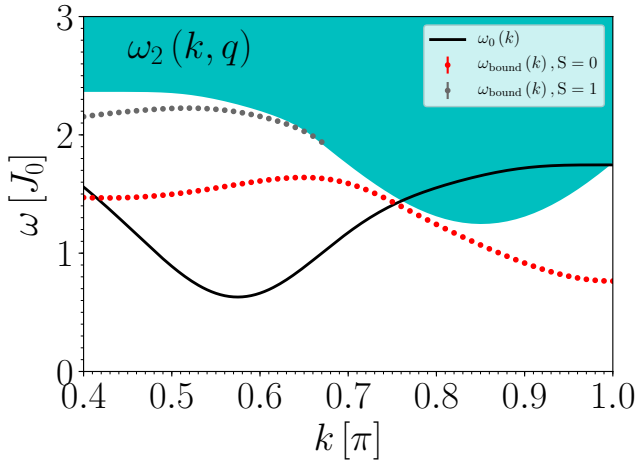


FIG. 3. **Isolated spin ladder** for $J_1 = 1.2J_0$ and $J_2 = 0.9J_1$: one-triplon dispersion in black, two-triplon scattering continuum is colored; the $S_{\text{tot}} = 0$ bound state is shown by the dotted red line and the $S_{\text{tot}} = 1$ bound state by the dotted grey line. Note that the wave number is given in units of π setting the lattice constant to unity. This corresponds to the reciprocal lattice units of BiCu_2PO_6 where the actual lattice constant is the distance between next-nearest neighbor rungs, cf. Refs. [2, 6].

ing the Hamiltonian is no longer sparse. In the previous trilinear case, the Hamiltonian relevant for the two-triplon subspace is diagonal. The triplon-triplon interaction, however, implies scattering between the states of all relative momenta so that the corresponding matrix is dense. We performed calculations for 40×8 \mathbf{k} -points. The results are shown in Fig. 4. Clearly, an additional branch with significant weight forks off the dispersion of the single dispersion at $k \approx 0.75$ r.l.u. with ≈ 7 meV. This agrees very well with the most prominent downturn in experiment. It provides evidence that two-triplon interactions and the concomitant binding are essential players in the physics of BiCu_2PO_6 . The bound state is not observed in experiment to 1 r.l.u. because it is an $S_{\text{tot}} = 0$ and visible only due to the DM terms. Beyond 0.8 r.l.u. its weight becomes very small [63].

Unfortunately, the resolution of the present calculation is not high enough to make a tangible statement about the second downturn at higher energy around 9.5 meV. It could result from a weaker bound state formed from triplons of different flavors. Note that the spin anisotropies split the triplons and hybridize them so that they acquire mixed flavors. An alternative and appealing explanation for the weak downturn at higher energies is suggested by the results for the trilinear model, see Fig. 2. While they do not explain the strong downturn at about 7 meV, it is possible that they explain the less pronounced downturn around 9.5 meV due to level repulsion [5]. The wave vector and the energy at which this downturn occurs agree between theory and experiment as well as the overall size of the feature. These observations call for future high-precision calculations including trilinear and quadrilinear terms. In this way, the intricate interplay between hybridization and attractive interaction in BiCu_2PO_6

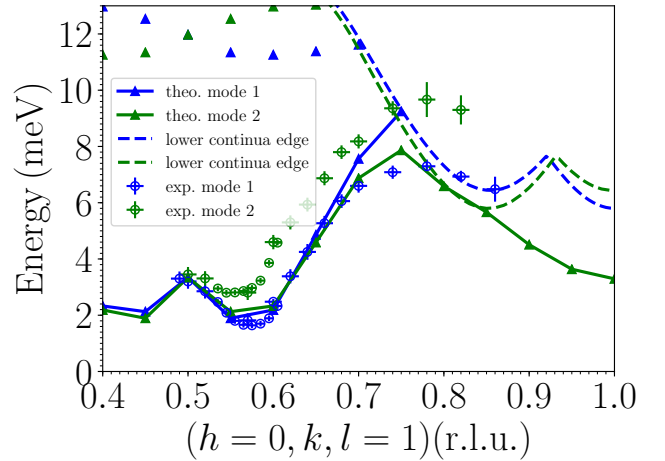


FIG. 4. **Energies in the quadrilinear model** for BiCu_2PO_6 for the parameters $J_0 = 8.0\text{meV}$, $J_1 = 1.2J_0$, $J_2 = 0.9J_1$, $J' = 0.16J_0$, $D_0^y = 0.1J_0$, $D_1^x = 0.25J_1$, $D_1^y = 0.38J_1$, $D_2^x = 0.0$, and $D_2^z = -0.06J_2$. The green (blue) dashed line shows the lower continuum edge derived from the theoretical dispersion displayed as green (blue) solid line. Unlinked symbols are the experimental data from Ref. [5, 62].

can be elucidated quantitatively. The lesson learned will provide the foundation for understanding many more strongly frustrated low-dimensional quantum antiferromagnets where tri- and quadrilinear processes need to be measured and understood.

IV. CONCLUSION

Summarizing, we analyzed the unusual dispersions found in BiCu_2PO_6 with respect to two important phenomena: decay and binding. Decay results from trilinear terms in second quantization formed by two creation and one annihilation operator or their hermitian conjugate representing fusion. Binding stems from quadrilinear terms formed by two creation and two annihilation operators. Generically, both types are present and their importance relative to the single-particle dispersion is particularly high in low-dimensional systems. BiCu_2PO_6 is a challenging exemplary system to study these fundamental processes because it hosts significant spin anisotropy terms so that different triplon flavors can be distinguished by their energy. In this system, evidence for the relevance of trilinear terms was found [5, 7]. Yet the strong, dominant downturn eluded an explanation. Our analysis including triplon-triplon interaction, i.e., with quadrilinear terms, suggests that the strong downturn is the signature of a $S = 0$ two-triplon bound state, slightly perturbed by the anisotropic terms so that it becomes visible in the dynamic structure factor measured by inelastic neutron scattering. The weak downturn at higher energies can be identified as the signature of level repulsion between a single triplon and the two-triplon continuum. These findings suggest BiCu_2PO_6 as a challenging exemplary platform to investigate the phenomena of binding and decay of

multi-flavor quasi-particles.

ACKNOWLEDGMENTS

This study was funded by the German Research Foundation (DFG) in grant UH 90/14-1. Parts of the calculations were

performed on the LiDO3 high-performance computing system funded by the DFG. We acknowledge useful discussions with Nils Drescher; he also provided the code to perform the CUT. We thank Carsten Nase for lasting technical support.

-
- [1] G. Schmiedinghoff, L. Müller, G. S. Uhrig, U. Kumar, and B. Fauseweh, Three-body bound states in antiferromagnetic spin ladders, *Comm. Phys.* **5**, 218 (2022).
- [2] A. A. Tsirlin, I. Rousochatzakis, D. Kasinathan, O. Janson, R. Nath, F. Weickert, C. Geibel, A. M. Läuchli, and H. Rosner, Bridging frustrated-spin-chain and spin-ladder physics: Quasi-one-dimensional magnetism of BiCu_2PO_6 , *Phys. Rev. B* **82**, 144426 (2010).
- [3] K. P. Schmidt and G. S. Uhrig, Excitations in one-dimensional $S = 1/2$ quantum antiferromagnets, *Phys. Rev. Lett.* **90**, 227204 (2003).
- [4] K. W. Plumb, Z. Yamani, M. Matsuda, G. J. Shu, B. Koteswararao, F. C. Chou, and Y.-J. Kim, Incommensurate dynamic correlations in the quasi-two-dimensional spin liquid BiCu_2PO_6 , *Phys. Rev. B* **88**, 024402 (2013).
- [5] K. W. Plumb, K. Hwang, Y. Qiu, L. W. Harriger, G. E. Granroth, A. I. Kolesnikov, G. J. Shu, F. C. Chou, C. Rüegg, Y. B. Kim, and Y.-J. Kim, Quasiparticle-continuum level repulsion in a quantum magnet, *Nat. Phys.* **12**, 224 (2016).
- [6] L. Splinter, N. A. Drescher, H. Krull, and G. S. Uhrig, Minimal model for the frustrated spin ladder system BiCu_2PO_6 , *Phys. Rev. B* **94**, 155115 (2016).
- [7] K. Hwang and Y. B. Kim, Theory of triplon dynamics in the quantum magnet BiCu_2PO_6 , *Phys. Rev. B* **93**, 235130 (2016).
- [8] L. P. Pitaevskii, Properties of the spectrum of elementary excitations near the disintegration threshold of the excitations, *Sov. Phys. JETP* **9**, 830 (1959).
- [9] B. Gaveau and L. S. Schulman, Limited quantum decay, *J. Phys. A* **28**, 7359 (1995).
- [10] M. E. Zhitomirsky, Decay of quasiparticles in quantum spin liquids, *Phys. Rev. B* **73**, 100404(R) (2006).
- [11] T. Fischer, S. Duffe, and G. S. Uhrig, Adapted continuous unitary transformation to treat systems with quasi-particles of finite lifetime, *New J. Phys.* **10**, 033048 (2010).
- [12] T. Fischer, *Description of quasiparticle decay by continuous unitary transformations* (TU Dortmund University, 44221 Dortmund, Germany, 2011).
- [13] M. E. Zhitomirsky and A. L. Chernyshev, Spontaneous magnon decays, *Rev. Mod. Phys.* **85**, 219 (2013).
- [14] R. Verresen, R. Moessner, and F. Pollmann, Avoided quasiparticle decay from strong quantum interactions, *Nat. Phys.* **15**, 750 (2019).
- [15] T. Hong, M. Matsumoto, Y. Qiu, W. Chen, T. R. Gentile, S. Watson, F. F. Awwadi, M. M. Turnbull, S. E. Dissanayake, H. Agrawal, R. Toft-Petersen, B. Klemke, K. Coester, K. P. Schmidt, and D. A. Tennant, Field-induced spontaneous quasiparticle decay and renormalization of quasiparticle dispersion in a quantum antiferromagnet, *Nat. Comm.* **8**, 15148 (2017).
- [16] J. Oh, M. D. Le, J. Jeong, J.-H. Lee, H. Woo, W.-Y. Song, T. G. Perring, W. J. L. Buyers, S.-W. Cheong, and J.-G. Park, Magnon Breakdown in a Two Dimensional Triangular Lattice Heisenberg Antiferromagnet of Multiferroic LuMnO_3 , *Phys. Rev. Lett.* **111**, 257202 (2013).
- [17] N. J. Robinson, F. H. L. Essler, I. Cabrera, and R. Coldea, Quasiparticle breakdown in the quasi-one-dimensional Ising ferromagnet CoNb_2O_6 , *Phys. Rev. B* **90**, 174406 (2014).
- [18] M. B. Stone, I. A. Zaliznyak, T. Hong, C. L. Broholm, and D. H. Reich, Quasiparticle breakdown in a quantum spin liquid, *Nature* **440**, 187 (2006).
- [19] T. Masuda, A. Zheludev, H. Manaka, L.-P. Regnault, J.-H. Chung, and Y. Qiu, Dynamics of Composite Haldane Spin Chains in IPA-CuCl_3 , *Phys. Rev. Lett.* **96**, 047210 (2006).
- [20] W. Zheng, J. O. Fjærestad, R. R. P. Singh, R. H. McKenzie, and R. Coldea, Excitation spectra of the spin- $\frac{1}{2}$ triangular-lattice Heisenberg antiferromagnet, *Phys. Rev. B* **74**, 224420 (2006).
- [21] A. L. Chernyshev and M. E. Zhitomirsky, Spin waves in a triangular lattice antiferromagnet: Decays, spectrum renormalization, and singularities, *Phys. Rev. B* **79**, 144416 (2009).
- [22] M. Mourigal, W. T. Fuhrman, A. L. Chernyshev, and M. E. Zhitomirsky, Dynamical structure factor of the triangular-lattice antiferromagnet, *Phys. Rev. B* **88**, 094407 (2013).
- [23] M. Mourigal, W. T. Fuhrman, A. L. Chernyshev, and M. E. Zhitomirsky, Erratum: Dynamical structure factor of the triangular-lattice antiferromagnet, *Phys. Rev. B* **93**, 099901(E) (2016).
- [24] M. Powalski, G. S. Uhrig, and K. P. Schmidt, Roton Minimum as a Fingerprint of Magnon-Higgs Scattering in Ordered Quantum Antiferromagnets, *Phys. Rev. Lett.* **115**, 207202 (2015).
- [25] M. Powalski, K. P. Schmidt, and G. S. Uhrig, Mutually attracting spin waves in the square-lattice quantum antiferromagnet, *SciPost Phys.* **4**, 1 (2018).
- [26] R. Verresen, F. Pollmann, and R. Moessner, Quantum dynamics of the square-lattice Heisenberg model, *Phys. Rev. B* **98**, 155102 (2018).
- [27] H. Bethe, Zur Theorie der Metalle. I. Eigenwerte und Eigenfunktionen der linearen Atomkette, *Z. Phys.* **71**, 205 (1931).
- [28] F. J. Dyson, General theory of spin-wave interactions, *Phys. Rev.* **102**, 1217 (1956).
- [29] J. Hanus, BOUND STATES IN THE HEISENBERG FERROMAGNET, *Phys. Rev. Lett.* **11**, 336 (1963).
- [30] M. Wortis, Bound States of Two Spin Waves in the Heisenberg Ferromagnet, *Phys. Rev.* **132**, 85 (1963).
- [31] J. Barker, U. Atxitia, T. A. Ostler, O. Hovorka, O. Chubykalo-Fesenko, and R. W. Chantrell, Two-magnon bound state causes ultrafast thermally induced magnetisation switching, *Sci. Rep.* **3**, 3262 (2013).
- [32] T. Oguchi and T. Ishikawa, Theory of Two-Magnon Bound States in a Two-Dimensional Antiferromagnet, *J. Phys. Soc. Jpn.* **34**, 1486 (1973).
- [33] C. J. Hamer, Energy spectrum of the two-magnon bound states in the Heisenberg-Ising antiferromagnet on the square lattice, *Phys. Rev. B* **79**, 212413 (2009).
- [34] S. Dusuel, M. Kamfor, K. P. Schmidt, R. Thomale, and J. Vidal, Bound states in two-dimensional spin systems near the Ising limit: A quantum finite-lattice study, *Phys. Rev. B* **81**, 064412

- (2010).
- [35] L. D. Faddeev and L. A. Takhtajan, What is the spin of a spin wave?, *Phys. Lett.* **85A**, 375 (1981).
- [36] M. Kohno, Dynamically Dominant Excitations of String Solutions in the Spin-1/2 Antiferromagnetic Heisenberg Chain in a Magnetic Field, *Phys. Rev. Lett.* **102**, 037203 (2009).
- [37] M. Ganahl, E. Rabel, F. H. L. Essler, and H. G. Evertz, Observation of Complex Bound States in the Spin-1/2 Heisenberg XXZ Chain Using Local Quantum Quenches, *Phys. Rev. Lett.* **108**, 077206 (2012).
- [38] Z. Wang, J. Wu, W. Yang, A. K. Bera, D. Kamenskyi, A. T. M. N. Islam, S. Xu, J. M. Law, B. Lake, C. Wu, and A. Loidl, Experimental observation of Bethe strings, *Nature* **554**, 219 (2018).
- [39] M. Greiter, Two-leg t - J ladder: A spin liquid generated by Gutzwiller projection of magnetic bands, *Phys. Rev. B* **65**, 134443 (2002).
- [40] M. Kohno, O. A. Starykh, and L. Balents, Spinons and triplons in spatially anisotropic frustrated antiferromagnets, *Nat. Phys.* **3**, 790 (2007).
- [41] D. G. Shelton, A. A. Nersisyan, and A. M. Tsvelik, Antiferromagnetic spin ladders: Crossover between spin $S = 1/2$ and $S = 1$ chains, *Phys. Rev. B* **53**, 8521 (1996).
- [42] O. P. Sushkov and V. N. Kotov, Bound states of magnons in the $s = 1/2$ quantum spin ladder, *Phys. Rev. Lett.* **81**, 1941 (1998).
- [43] S. Trebst, H. Monien, C. J. Hamer, Z. Weihong, and R. R. P. Singh, Strong-coupling expansions for multiparticle excitations: Continuum and bound states, *Phys. Rev. Lett.* **85**, 4373 (2000).
- [44] C. Knetter, K. P. Schmidt, M. Grüninger, and G. S. Uhrig, Fractional and integer excitations in quantum antiferromagnetic spin 1/2 ladders, *Phys. Rev. Lett.* **87**, 167204 (2001).
- [45] M. Windt, M. Grüninger, T. Nunner, C. Knetter, K. P. Schmidt, G. S. Uhrig, T. Kopp, A. Freimuth, U. Ammerahl, B. Büchner, and A. Revcolevschi, Observation of two-magnon bound states in the two-leg ladders of $(\text{Ca},\text{La})_{14}\text{Cu}_{24}\text{O}_{41}$, *Phys. Rev. Lett.* **87**, 127002 (2001).
- [46] K. P. Schmidt and G. S. Uhrig, Spectral properties of magnetic excitations in cuprate two-leg ladder systems, *Mod. Phys. Lett. B* **19**, 1179 (2005).
- [47] S. Notbohm, P. Ribeiro, B. Lake, D. A. Tennant, K. P. Schmidt, G. S. Uhrig, C. Hess, R. Klingeler, G. Behr, B. Büchner, M. Reehuis, R. I. Bewley, C. D. Frost, P. Manuel, and R. S. Eccleston, One- and two-triplon excitations of an ideal spin-ladder, *Phys. Rev. Lett.* **98**, 027403 (2007).
- [48] A. M. Tsvelik, Spectrum of magnetic excitations in the spin-Peierls state, *Phys. Rev. B* **45**, 486 (1992).
- [49] G. S. Uhrig and H. J. Schulz, Magnetic excitations spectrum of dimerized antiferromagnetic chains, *Phys. Rev. B* **54**, R9624 (1996).
- [50] G. S. Uhrig and H. J. Schulz, Erratum: "Magnetic excitations spectrum of dimerized antiferromagnetic chains", *Phys. Rev. B* **58**, 2900(E) (1998).
- [51] K. P. Schmidt, C. Knetter, and G. S. Uhrig, Spectral properties of the dimerized and frustrated $S = 1/2$ chain, *Phys. Rev. B* **69**, 104417 (2004).
- [52] C. Knetter, A. Bühler, E. Müller-Hartmann, and G. S. Uhrig, Dispersion and Symmetry of Bound States in the Shastry-Sutherland Model, *Phys. Rev. Lett.* **85**, 3958 (2000).
- [53] P. Lemmens, M. Grove, M. Fischer, G. Güntherodt, V. N. Kotov, H. Kageyama, K. Onizuka, and Y. Ueda, Collective Singlet Excitations and Evolution of Raman Spectral Weights in the 2D Spin Dimer Compound $\text{SrCu}_2(\text{BO}_3)_2$, *Phys. Rev. Lett.* **85**, 2605 (2000).
- [54] C. Knetter and G. S. Uhrig, Dynamic Structure Factor of the Two-Dimensional Shastry-Sutherland Model, *Phys. Rev. Lett.* **92**, 027204 (2004).
- [55] O. Mentré, E. M. Ketatni, M. Colmont, M. Huve, F. Abraham, and V. Petricek, Structural Features of the Modulated $\text{BiCu}_2(\text{P}_{1-x}\text{V}_x)\text{O}_6$ Solid Solution; 4-D Treatment of $x = 0.87$ Compound and Magnetic Spin-Gap to Gapless Transition in New Cu^{2+} Two-Leg Ladder Systems, *Journal of the American Chemical Society* **128**, 10857 (2006).
- [56] S. Wang, E. Pomjakushina, T. Shiroka, G. Deng, N. Nikseresht, C. Rüegg, H. M. Rønnow, and K. Conder, Crystal growth and characterization of the dilutable frustrated spin-ladder compound $\text{Bi}(\text{Cu}_{1-x}\text{Zn}_x)_2\text{PO}_6$, *J. Cryst. Growth* **313**, 51 (2010).
- [57] T. Moriya, Anisotropic superexchange interaction and weak ferromagnetism, *Phys. Rev.* **120**, 91 (1960).
- [58] L. Shekhtman, O. Entin-Wohlman, and A. Aharony, Moriya's anisotropic superexchange interaction, frustration, and Dzyaloshinsky's weak ferromagnetism, *Phys. Rev. Lett.* **69**, 836 (1992).
- [59] C. Knetter and G. S. Uhrig, Perturbation theory by flow equations: dimerized and frustrated $S = 1/2$ chain, *Eur. Phys. J. B* **13**, 209 (2000).
- [60] H. Krull, N. A. Drescher, and G. S. Uhrig, Enhanced perturbative continuous unitary transformations, *Phys. Rev. B* **86**, 125113 (2012).
- [61] S. Sachdev, Quantum magnetism and criticality, *Nat. Phys.* **4**, 173 (2008).
- [62] K. W. Plumb, K. Hwang, Y. Qiu, L. W. Harriger, G. E. Granroth, G. J. Shu, F. C. Chou, C. Rüegg, Y. B. Kim, and Y.-J. Kim, Giant Anisotropic Interactions in the Copper Based Quantum Magnet BiCu_2PO_6 , arXiv:1408.2528v1 (2014).
- [63] L. B. Müller, *Quasiparticle decay induced by spin anisotropies in the frustrated spin ladder system BiCu_2PO_6* (TU Dortmund University, 442121 Dortmund, Germany, 2021).

Appendix A: Technical Details

The dynamic structure factor in the time domain reads

$$S^{\alpha\beta}(\mathbf{q}, \omega) = \frac{1}{2\pi} \int_{-\infty}^{\infty} dt e^{i\omega t} \langle S^\alpha(-\mathbf{q}, t) S^\beta(\mathbf{q}, 0) \rangle. \quad (\text{A1})$$

At zero temperature, its Fourier transform for $\alpha = \beta$ is given by the retarded Green function

$$G^{\text{ret},\alpha}(\mathbf{q}, \omega) = \langle u_0 | \frac{1}{\omega - H(\mathbf{q})} | u_0 \rangle, \quad (\text{A2})$$

where $|u_0\rangle = S^\alpha(\mathbf{q}, 0)|0\rangle$ with $|0\rangle$ being the ground state. We omit α henceforth since we focus on the energies and not on the spectral weights here.

The action of the Hamiltonian in (A2) is represented by a tridiagonal matrix

$$\bar{H}(\mathbf{q}) = \begin{pmatrix} a_0(\mathbf{q}) & b_1(\mathbf{q}) & 0 & 0 & \cdots \\ b_1(\mathbf{q}) & a_1(\mathbf{q}) & b_2(\mathbf{q}) & 0 & \cdots \\ 0 & b_2(\mathbf{q}) & a_3(\mathbf{q}) & b_3(\mathbf{q}) & \cdots \\ \vdots & \vdots & \vdots & \vdots & \ddots \end{pmatrix} \quad (\text{A3})$$

which is computed by Lanczos iteration

$$|u_1\rangle = (H(\mathbf{q}) - a_0(\mathbf{q}))|u_0\rangle \quad (\text{A4a})$$

$$|u_2\rangle = (H(\mathbf{q}) - a_1(\mathbf{q}))|u_1\rangle - b_1^2(\mathbf{q})|u_0\rangle \quad (\text{A4b})$$

$$|u_3\rangle = (H(\mathbf{q}) - a_2(\mathbf{q}))|u_2\rangle - b_2^2(\mathbf{q})|u_1\rangle \quad (\text{A4c})$$

...

yielding the coefficients

$$a_i(\mathbf{q}) = \frac{\langle u_i | H(\mathbf{q}) | u_i \rangle}{\langle u_i | u_i \rangle} \quad \text{for } i = 0, 1, 2, \dots \quad (\text{A5a})$$

$$b_i^2(\mathbf{q}) = \frac{\langle u_i | u_i \rangle}{\langle u_{i-1} | u_{i-1} \rangle} \quad \text{for } i = 1, 2, 3, \dots \quad (\text{A5b})$$

$$b_0(\mathbf{q}) = 0. \quad (\text{A5c})$$

Finally, the Green function is computed by its continued fraction down to a certain depth of 30 to 100 fractions

$$G^{\text{ret}}(\mathbf{q}, \omega) = \frac{1}{\omega - a_0(\mathbf{q}) - \frac{b_1^2(\mathbf{q})}{\omega - a_1(\mathbf{q}) - \frac{b_2^2(\mathbf{q})}{\omega - a_2(\mathbf{q}) - \dots}}}, \quad (\text{A6})$$

Then, the continued fraction is terminated by the square root terminator

$$T(\mathbf{q}, \omega) = \frac{1}{2b_\infty^2(\mathbf{q})} \left(\omega - a_\infty(\mathbf{q}) - \sqrt{R(\mathbf{q}, \omega)} \right) \quad \text{for } \omega \geq \omega_{2,\text{max}}(\mathbf{q}) \quad (\text{A7a})$$

$$T(\mathbf{q}, \omega) = \frac{1}{2b_\infty^2(\mathbf{q})} \left(\omega - a_\infty(\mathbf{q}) - i\sqrt{-R(\mathbf{q}, \omega)} \right) \quad \text{for } \omega_{2,\text{min}} \leq \omega \leq \omega_{2,\text{max}}(\mathbf{q}) \quad (\text{A7b})$$

$$T(\mathbf{q}, \omega) = \frac{1}{2b_\infty^2(\mathbf{q})} \left(\omega - a_\infty(\mathbf{q}) + \sqrt{R(\mathbf{q}, \omega)} \right) \quad \text{for } \omega \leq \omega_{2,\text{min}}(\mathbf{q}), \quad (\text{A7c})$$

where we used

$$\omega_{2,\text{min}}(\mathbf{q}) = a_\infty(\mathbf{q}) - 2b_\infty(\mathbf{q}) \quad (\text{A8a})$$

$$\omega_{2,\text{max}}(\mathbf{q}) = a_\infty(\mathbf{q}) + 2b_\infty(\mathbf{q}) \quad (\text{A8b})$$

and

$$R(\mathbf{q}, \omega) = (\omega - a_\infty(\mathbf{q}))^2 - 4b_\infty^2(\mathbf{q}). \quad (\text{A9})$$

Appendix B: Dispersion in the bilinear model

An overview of the dispersion in the bilinear model including the description of all technical aspects is provided in Ref. [6]. For comparison to the dispersions on the trilinear and on the quadrilinear level we include here the bilinear data in Fig. 5. The theoretical fits agree well with the experimental data, but the bilinear theory does not capture any feature like the downturns. They require to consider models beyond the bilinear level.

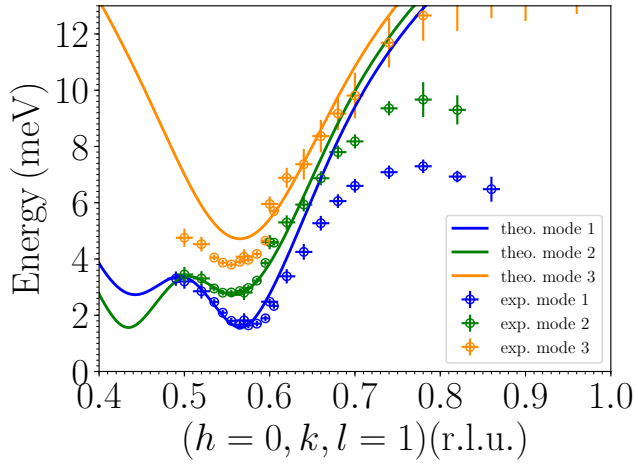


FIG. 5. **Energies in the bilinear model** for BiCu_2PO_6 for the parameters $J_0 = 9.4\text{meV}$, $J_1 = 1.2J_0$, $J_2 = 0.9J_1$, $J' = 1.5\text{meV}$, $D_0^y = 0$, $D_1^x = 0.48J_1$, $D_1^y = 0.61J_1$, $D_2^x = 0$, and $D_2^z = -0.02J_2$. Unlinked symbols are the experimental data from Ref. [5, 62].